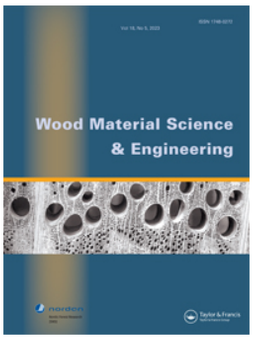

Wood Material Science & Engineering

ISSN: (Print) (Online) Journal homepage: https://www.tandfonline.com/loi/swoo20

Wood fiber production from downed timber for manufacturing wood polymer composite: fiber property characterization

Yucheng Peng, Dikshya Pokhrel, Xueqi Wang, Thomas Elder, Nicole Stark, Brian Via, Tom Gallagher, Mathew Smidt & Dana Mitchell

To cite this article: Yucheng Peng, Dikshya Pokhrel, Xueqi Wang, Thomas Elder, Nicole Stark, Brian Via, Tom Gallagher, Mathew Smidt & Dana Mitchell (29 Oct 2023): Wood fiber production from downed timber for manufacturing wood polymer composite: fiber property characterization, Wood Material Science & Engineering, DOI: 10.1080/17480272.2023.2266832

To link to this article: https://doi.org/10.1080/17480272.2023.2266832

Published online: 29 Oct 2023.

WOOD MATERIAL SCIENCE & ENGINEERING
https://doi.org/10.1080/17480272.2023.2266832

Taylor & Francis
Taylor & Francis Group

ORIGINAL ARTICLE

Wood fiber production from downed timber for manufacturing wood polymer composite: fiber property characterization

Yucheng Peng[a], Dikshya Pokhrel[a], Xueqi Wang[a], Thomas Elder[b], Nicole Stark[c], Brian Via[a], Tom Gallagher[a], Mathew Smidt[b] and Dana Mitchell[b]

[a]College of Forestry, Wildlife, and Environment, Auburn University, Auburn, AL, USA; [b]USDA-Forest Service, Southern Research Station, Auburn, AL, USA; [c]USDA-Forest Service, Forest Products Laboratory, Madison, WI, USA

ABSTRACT

Massive amount of downed timber is generated by hurricanes and tornados. This research studied the properties of wood fibers (WFs) generated from downed loblolly pine (*Pinus taeda* L.) trees at different maturity (ages 15, 30, and 39 years) with various natural environmental exposure periods (0, 6, and 12 months) for wood polymer composite (WPC) manufacturing. The wood fiber critical properties for WPC manufacturing, including particle size and morphologies, physical and chemical properties, and thermal stability, were characterized. Prolonged environmental exposure increased WF surface roughness. The density and 1% sodium hydroxide solubility of WFs for the 15 – and 30-year-old tree decreased after 12 months of environmental exposure. The WFs generated from the 39-year-old tree contain extractives due to heartwood development, resulting in significantly less moisture absorption. Thermogravimetric analysis results showed no significant change in the thermal stability of WFs generated from the 15 – and 30-year-old trees after natural environmental exposure because of the loss of degraded wood components. The cellulose and lignin thermal degradation peak temperatures decreased by up to 9 and 6 °C for WFs extracted from the 39-year-old tree. The degraded wood components were fixed within WFs due to extractives, causing thermal degradation peak temperatures to decrease.

ARTICLE HISTORY
Received 24 June 2023
Accepted 1 October 2023

KEYWORDS
EWPs; timber; environmental exposure; particle size distribution; sodium hydroxide solubility

Introduction

The southeastern United States has one of the most abundant timber supplies and active markets (Prestemon and Holmes 2010, Rutledge *et al.* 2021). However, frequent weather events like tornadoes and hurricanes in this region threaten these timber resources and damage millions of acres of forest land (Prestemon and Holmes 2010). Hurricane Katrina in 2005 damaged five million acres (~ 40%) of the forest land in the state of Mississippi. The timber loss was estimated to be 125 million tons, equivalent to five years of annual harvests (Kupfer *et al.* 2008, Yao *et al.* 2022). Hurricane Nate in 2017 damaged about 5% of the forest cover in Mississippi (Yao *et al.* 2022). Hurricane Michael, in 2018, destroyed over three million acres of forest land in Florida with an estimated timber value of over $1 billion. The storm also damaged more than two million acres of forest land in Georgia, with an estimated timber loss of more than $762 million. The recent hurricane Zeta in October 2020 caused $4.4 billion in damage in Louisiana, Mississippi, Alabama, and Georgia (Yao *et al.* 2022). The damage to the forest land has not been estimated, but significant damage to forest land along the hurricane's path was reported.

Such severe wind events kill trees by breaking or uprooting them and weaken residual trees. Trees that survive these natural disturbances may be of lower quality because of deformations to their boles or degradation of wood from insect damage, fungal decay, or injury-triggered mineral stain (Radtke *et al.* 2004, Long *et al.* 2005, Vogt *et al.* 2020). Fiber kinking and deformation may also occur in the lower-outer portion of surviving trees, due to possible wind forces at the crown and likely this will occur to standing trees just before they are downed in the hurricane (Via *et al.* 2006). The volume of downed timber generated due to severe wind events is several times higher than the annual harvest volume (Stanturf *et al.* 2007, Mitchell *et al.* 2021). Harvesting the downed timber is challenging due to its high volume, limited harvesting window, available logging equipment, human resources, and worker safety concerns during operation (Aghalari *et al.* 2021). Therefore, a rapid harvesting operation is difficult, and trees may be left on site for a relatively long time, leading to wood fiber quality degradation.

Generally, the degradation of wood progresses through several stages with prolonged exposure to the natural environment (Wong and Wilkes 1988, Blanchette *et al.* 1997, Eastwood 2014, Ayrilmis *et al.* 2015). Fungi mainly cause wood quality degradation. Brown rot, white rot, and soft rot are the three primary fungi most reported to be responsible for wood degradation. Brown rot fungi mostly affect softwoods and are active above ground. They depolymerize cellulose, leaving a lignin-rich substrate (Broda and Popescu 2019). White rot fungi cause uniform degradation of carbohydrates and lignin simultaneously. It also causes selective degradation of lignin over hemicelluloses components (Blanchette *et al.* 1997, Pandey and Pitman 2003, Ayrilmis *et al.* 2015). Soft rot degrades

CONTACT Yucheng Peng yzp0027@auburn.edu College of Forestry, Wildlife, and Environment, Auburn University, 602 Duncan Drive, Auburn, AL 36849, USA

carbohydrates in preference to lignin, causing significant strength losses in the wood (Broda and Popescu 2019). In the field, any of the three degradation rot mechanisms can occur, making it challenge to control and interpret for experimental purposes.

In the wood structure, hemicellulose is a low molecular weight carbohydrate, which is the first component to be degraded when left in the environment. This is a critical stage during fungal degradation because cellulose microfibrils are surrounded by hemicellulose (Pandey and Pitman 2003, Funda *et al.* 2020). In the early stage of fungal degradation, the strength of wood decreases without significant weight loss. The strength loss is mainly caused by the degradation of galactan and arabinan components in the hemicellulose (Curling *et al.* 2002, Mott *et al.* 2002, Groom *et al.* 2002a, Groom *et al.* 2002b). In a later stage of decay, significant weight loss occurs due to the loss of mannan and xylan in hemicellulose. Initial extensive weight loss is characterized by hemicellulose degradation due to the loss of glucan components (Curling *et al.* 2001). Cellulose degradation follows and lowers the stiffness of the wood fibers further. The intensive loss in stiffness in the wood is mainly due to the loss of the glucan component in cellulose rather than in hemicellulose during the decay progression (Curling *et al.* 2001, Curling *et al.* 2002).

Another major factor affecting decay progression in downed timber is the age of the tree (juvenile versus mature wood), characterized by varying amounts of cell wall components, including cellulose, hemicellulose, and lignin (Wong and Wilkes 1988, Blanchette *et al.* 1997). A 15-year-old tree contains about 85% juvenile wood, while a 40-year-old tree has only about 15% of juvenile wood (Yeh 2006). Juvenile wood is rich in lignin and contains less cellulose, while mature wood contains more cellulose. Juvenile wood also has lower wood density, shorter fiber lengths, and much higher microfibril angles. The higher microfibril angle results in lower fiber stiffness and significantly reduced strength due to plastic deformation in the adjacent and thicker lignin sheath (Via *et al.* 2007, Via *et al.* 2009). Due to the higher microfibril angle and lower density, the strength properties of juvenile wood are lower than that of mature wood. Since the overall properties of wood are variable (Mcmillin 1968, Knoll *et al.* 1993b, Yeh 2006) the changes in physical and chemical properties due to the exposure to the natural environment of the downed timber at different ages are also expected to differ.

The wood-water relation under degradation conditions is another crucial factor altering the wood properties. Hemicellulose absorbs moisture from the environment due to its amorphous structure. When wood degrades, hemicellulose is lost, and with the loss of accessible hydroxyl groups, wood fibers are expected to absorb less moisture from the environment. The amorphous regions in cellulose also change during the initial degradation stage, which changes the crystalline structure of the wood fibers, leading to different moisture absorption behaviors (Hastrup *et al.* 2012, Eastwood 2014, Ayrilmis *et al.* 2015). Simultaneously, the moisture absorption property impacts the mechanical behaviors of wood fibers. Hehar et al. found that the moisture content of wood fibers affected the number of fine particles generated during the wood fiber size reduction process (Hehar *et al.* 2014). Higher moisture content in wood results in longer grinding times, generating more fine particles. Lower moisture content required less energy to break the wood fibers, and more large particles were generated. Additionally, the change in the crystalline structure of cellulose due to degradation altered the brittleness of wood, resulting in different behavior during the milling or grinding of wood into fibers. The effect of the degradation on the wood-water relation of downed timber needs to be investigated.

Simultaneously, downed timber exposed to the natural environment is also attacked by insects and pests (Radtke *et al.* 2004, Lindenmayer *et al.* 2008), which is site dependent. Therefore, the degradation of downed timber is complex and varies by site, tree age, soil type, moisture, relative humidity (RH), temperature, and precipitation following the hurricane (Radtke *et al.* 2004, Lindenmayer *et al.* 2008). In addition, when downed timber is harvested soon after a weather event, salvage harvesting leads to overstocking in the wood processing facilities (Prestemon and Holmes 2004, Kupfer *et al.* 2008, Aghalari *et al.* 2021, Mitchell *et al.* 2021). Exploring the applications of downed timber in various fields like energy generation, pulp production, particle and fiber board manufacturing, and structural members of construction is thus an environmentally sustainable approach to minimize environmental and economic loss. This study examined the potential of generating wood fibers from downed timber for manufacturing wood polymer composites and this part focused on characterization of wood fibers generated. The quality of downed timber and its fibers changes with time as the downed timber is exposed to environmental conditions. Insights associated with the time during which the downed timber needs to be collected for generating wood fibers to manufacture wood polymer composite are provided in this study. Using downed timber by the wood composite industry also fulfills their increasing raw material needs and opens a new market for downed timber utilization. With the high temperatures and high RH, and potential for rapid degradation in the southeastern US, the quality of the downed timber needs to be evaluated before commercial applications.

This study aims to understand the process of generating wood fibers from downed timber and the characterization of wood fiber properties related to wood polymer composite manufacturing. For wood polymer composite manufacturing, the fiber morphologies, particle size distribution, chemical characteristics, and thermal behaviors are important and were evaluated for the wood fibers from downed timber (Elsheikh *et al.* 2022). To simulate the downed timber, trees of selected ages were felled and stored onsite in the natural environment for sample collection at different periods (0, 6, and 12 months). The one-year environmental exposure time was selected based on the hurricane occurrence cycle of one year. The logs were then cut into blocks for chipping and milling to generate wood fibers. The effects of different tree ages and environmental exposure times on wood fiber morphological, physical, chemical, and thermal properties were characterized.

Materials and methods

Materials

Trees damaged by hurricanes or extreme weather events occur in all ages. In this study, three loblolly pine (*Pinus taeda* L.) trees at the ages of 15, 30, and 39 years old (denoted as L15, L30, and L39, respectively) were cut at the Solon Dixon Forestry Education Center, Andalusia, AL, October 22, 2020, based on the resource availability. The first batch, 0-month (denoted as 0M) log samples about 15–30 cm long, was collected on November 3, 2020, right above the stump (~ 30 cm). The remaining parts of all the trees were left on the forest floor with exposure to the natural environment. After six months of environmental exposure, the second batch of log samples (denoted as 6M) around 15–30 cm long was collected from the bottom part of the trees on April 23, 2021. The third batch of log samples (denoted as 12M) was collected from the bottom end of the remaining trees on October 1, 2021. The log samples collected at 0M, 6M, and 12 M were brought to the laboratory immediately after collection and stored in a freezer at – 20 °C. The sample is then named by a combination of the tree age and collection time; for example, L15-0M represents the sample with the tree age of 15 years collected at the first month when the tree was felled. Detailed information about the trees and their geographical locations is shown in Table 1. The tree diameter at breast height was measured using a tape measure before felling. Required chemicals, including sodium hydroxide (NaOH) and acetic acid, were obtained from VWR International (Radnor, PA, USA) and Millipore Sigma (St. Louis, MO, USA), respectively.

Wood fiber preparation

Wood fibers were generated from the collected log samples in three steps. The log samples were first reduced in size in preparation for the chipping operation. Bark was removed from the logs, followed by log size reduction into discs using a chainsaw. The wood discs were further reduced into wood blocks with maximum dimensions of $76 \times 127 \times 254$ mm to be fed through a chipper. The chipping operation was performed using a 12.7×8.9-cm 457cc Brush Master chipper shredder CH11 (Maple Grove, MN, USA). Then the wood chips with approximate dimensions of $12.7 \times 12.7 \times 25.4$ mm were milled using a Thomas Wiley Laboratory Mill-Model 4 (Model no. 3375-E20, Thomas Scientific, Swedesboro, NJ, USA) using a 2 mm screen. The blade rotation speed of 1725 revolutions per minute (rpm) was used during the milling. The final step of generating wood fibers in different particle sizes was performed on a Thomas Wiley Mini-Mill (Model no. 3383-L10, Thomas Scientific, Swedesboro, NJ, USA) using two different screens: a 40 and a 60-mesh. A blade rotation speed of 800 rpm was used for the final milling process. Prior to milling, wood chips were dried at 105 °C to a constant weight. After production, the wood fibers were stored in air-tight Ziploc plastic bags in the freezer.

Table 1. Information about the sample trees.

Tree	Age	Geographical location	Tree Height (m)	Diameter at breast height (dbh) (cm)	Stump Height (cm)	Length of sampling log (cm)
L39	39	31° 08′ 09″ N 86° 42′ 00″ W	26.7	53.3	30	15 - 30
L30	30	31° 08′ 19″ N 86° 40′ 19″ W	19.8	41.9	30	15 - 30
L15	15	31° 08′32″ N 86° 40′ 09″ W	19.2	25.4	30	15 - 30

Density and ash content measurement

The density of the wood was measured by following a modified procedure specified in ASTM D2395 with approximately 10 g of wood chips. The ash content of wood fibers was determined using ASTM D1102-84 (2021) to measure the amount of ash (%) that remained after dry oxidation at 600 °C. Approximately 2 g oven-dried wood fibers that passed through a 60-mesh sieve were weighted in a crucible which was placed in a muffle furnace (Thermolyne, Thermo Scientific, Dubuque, IA, USA) at 600 °C for six hours. The crucibles with their residues were immediately transferred from the furnace to a desiccator, and the ash was weighed after cooling. Then the crucible with ash was again heated in the muffle furnace at 600 °C for another 30-min period until the weight after cooling was constant, with the weight difference less than 0.2 mg. The ash content measurement was conducted in three replicates.

Wood fiber morphology characterization

Milled wood fibers using a 60-mesh screen during the milling process were examined using a stereomicroscope (Model No: 420T-1107, Boreal Science, Ontario, Canada) equipped with WF10 x eyepieces with objective lens up to 4 x magnification. Images of the wood fibers were captured using a C-mount-ready camera (Moticam 1080, Motic Scientific, Schertz, TX, USA) with a fitted video adaptor using Moticam 3.0 software. Microscopic images of the wood fibers with 40 times magnification were captured.

Particle size analysis

The particle size distribution of the wood fiber samples milled down to 60-mesh was characterized using sieve analysis. Sieving was performed using a mechanical sieve shaker Humboldt Model no. H-4330 (Elgin, IL, US) with brass sieves, 20-cm diameter and 5-cm depth from Advantech Manufacturing, Inc. (New Berlin, WI, US). Sieves of the US standard mesh sizes 140 (106 μm), 100 (150 μm), 80 (180 μm), 60 (250 μm), and 40 (425 μm) were stacked on top of each other. A sample of approximately 25 g was placed on the top sieve of size 40. A bottom pan was placed beneath the sieve of mesh size 140 to allow passing particles to be collected. The shaker kept running for 20 min with a motor rotation of 1725rpm. The wood fiber mass bracketed between two sieves represented a wood fiber size which was weighed and recorded. The sieve analysis was repeated three times for each sample to obtain a statistical representation of the size of the wood fibers.

Fourier transformation infrared spectroscopy (FT-IR)

After milling, fibers generated using a 60-mesh screen were analyzed by FT-IR using a PerkinElmer Spotlight 400 FT-IR/FT-NIR spectrometer (Waltham, MA, USA) accompanied by an ATR accessory with Diamond/ZnSe crystal. Background spectra were collected for each sample run. The spectra for each wood fiber sample were collected from 650 to 4000 cm^{-1} with 64 scans in a 4 $cm - ^{1}$ resolution. Three replicates were performed on each sample. The data analysis was performed using Spectrum 6 Spectroscopy Software (PerkinElmer, Massachusetts, USA).

Sodium hydroxide solubility

The 1% sodium hydroxide solubility test was performed in accordance with ASTM D1109. About 2 g of dried wood fibers after milling using 40 mesh screen were used for the test. The wood fibers were first placed in a 200-ml, tall-form beaker to which 100 ml of 1% NaOH solution was added. After mixing the NaOH solution and wood fibers by stirring, the beaker was placed in a hot water bath (100 °C) for one hour. During the heating process, the beaker top was covered by aluminum foil to prevent evaporation. Periodic stirring of the contents inside the beaker was carried out three times at 10, 15, and 25 min after the beaker was placed in the water bath. At the end of one hour, the contents of each beaker were filtered into tared crucibles. The wood fibers were washed with 100 ml of hot water, followed by 50 ml of 10% acetic acid by volume, and then thoroughly washed with hot water. The wood fibers were recovered after washing by filtration and dried to a constant weight. The difference in weight after the extraction process was reported and three replicates were obtained for each sample.

Equilibrium moisture content (EMC)

The EMC values of the wood fibers at 35 °C and RH levels of 35, 45, 60, 75, and 90% were measured to investigate the effect of tree age and environmental exposure time on moisture adsorption property. For each wood sample, three milled specimens of around 10 g, obtained from milling using a 2 mm screen, were used after oven drying to a constant weight at 105 °C. The wood particles were then placed in an environmental chamber of Memmert HCP 108 (Memmert GmbH + Co. KG, Germany) at the specific temperature and RH. The selected measurement temperature and RH levels were based on the capability of the environmental chamber. The weight of each sample was measured every 24 h until it reached a constant value. The moisture gain (%) was recorded at an initial RH of 35%. Once the equilibrium was achieved at 35% RH, the sample was then sequentially conditioned to the RH of 45, 60, 75, and 90% at the same temperature. The EMC of the wood fiber samples was calculated and reported as an average of three measurements on a dry basis.

Thermogravimetric analysis (TGA)

The thermal behaviors of the wood fibers were characterized using a TA Instruments Q50 (TA Instruments, DL, USA) thermogravimetric analysis system. Approximately 20 - 30 mg of milled wood that were obtained by milling with a 40-mesh screen were used for the analyses. Samples were loaded onto a platinum pan and heated from ambient temperature to 800 °C in a nitrogen atmosphere with a gas flow rate of 60 ml/min using a temperature ramp rate of 10 °C /minute. Each sample was tested twice.

Statistical analysis

Statistical analysis was performed on the data generated in density, ash content, particle size distribution, FTIR signals, 1% NaOH solubility, and EMC to understand the effect of the two factors: tree age and environmental exposure time. A two-way analysis of variance (ANOVA) with a 0.05 significance level was performed. A statistical model was used to represent the mean value of the property data of the milled wood fibers impacted by the two factors of tree age (α) and environmental exposure time (β), as shown in equation (1) (Peng *et al.* 2012).

$$Y_{ijk} = \mu + \alpha_i + \beta_j + (\alpha\beta)_{ij} + e_{ijk} \quad (1)$$

where i = 1, 2, 3; j = 1, 2, 3; and k = 1, 2, 3. Y_{ijk} is the mean property of the wood fibers measured, and μ is the population mean property of the wood fibers. The effect of tree age and environmental exposure time on the wood fiber property is represented by α_i and β_j. Effects of the interactions between the two factors are symbolized as $(\alpha\beta)_{ij}$. The errors in this model (e_{ijk}) were assumed to be independently, identically, and normally distributed. Following the ANOVA analysis, a *post-hoc* test using Tukey's Honestly Significant Difference (TukeyHSD) test was used to measure the effect of different levels within each factor group.

Results and discussion

Density and ash content

The basic densities of the wood samples are shown in Table 2. The densities at 0M for L15, L30, and L39 are 550, 580, and 570 kg/m^3, respectively. After six months of exposure to the natural environment, the densities for the three trees decreased slightly to 540, 560, and 550 kg/m^3 for L15, L30, and L39, respectively. The two-way ANOVA analysis indicated that a statistically significant difference in wood density was observed by tree age ($F(\alpha) = 3.88$, $P = 0.0397 < 0.05$) and environmental exposure time ($F(\beta) = 12.569$, $p < 0.001$), though the interaction between tree age and environmental exposure time was not significant. A Tukey *post-hoc* test revealed that no significant density difference was observed with different ages for samples collected at zero month environmental exposure. There is no statistically significant decrease in wood density for the first six months of

Table 2. Density of trees at different exposure times.

	Density (kg/m^3)		
Sample ID	0M	6M	12M
L15	550 ± 2	540 ±3	460 ± 4
L30	580± 3	560 ± 2	500 ± 2
L39	570 ±3	550 ± 2	540 ± 4

environmental exposure for all the wood samples. After 12 months of exposure, the densities for the three log samples decreased to 460, 500, and 540 kg/m^3, or approximately 16%, 14%, and 5% for L15, L30, and L39, respectively. During natural environmental exposure, the younger trees lost more mass due to degradation and weathering, resulting in a larger density decrease. The Tukey *post-hoc* test indicated that the wood density of L15 and L30 significantly decreased with 12 months of environmental exposure while the density of L39 did not change significantly. The older tree (L39) in which heartwood had formed, could be more durable when exposed to the environment. The extractives of heartwood in the L39 sample can be confirmed in the FT-IR spectra, 1% sodium hydroxide solubility data, and the TGA analysis results covered in later sections.

The ash content data for all the wood fibers are shown in Table 3. The interaction between tree age and environmental exposure time ($F = 4.45$, $p = 0.011 < 0.05$) significantly impact the ash content of wood fibers. The ash content of the younger tree (L15) is slightly greater than the other two, consistent with observations from the literature (McMillin 1968a). When the wood fibers were exposed to the natural environment for degradation, the statistical analysis showed that the ash content increased significantly (Table 3). The increase in ash content for the log samples with the prolonged storage time in the environment is related to the loss of volatile matter, low molecular weight cell wall components, and degradation products of wood cell wall components (Oyedeji *et al.* 2016).

Wood fiber morphology and particle size distribution

The morphologies of wood fibers were observed using a light microscope, and the images of these wood fibers are shown in Figure 1. The wood fibers were generated using a cutting mill, and different sizes of wood fibers were obtained within each sample. During the milling process, the blade cuts the large wood particles into smaller sizes, and the friction between wood fibers inside the milling chamber also helps to reduce the wood particle size. The wood fibers with the least dimension smaller than 60-mesh screen opening (250 µm) were collected for characterization. The maximum dimension of wood fibers that can go through the screen opening in the diagonal direction is around 350 µm. Wood fibers in slender shapes with aspect ratios (the largest dimension divided by the smallest dimension observed in the images) greater than one were mostly observed. Large wood particles with widths and lengths up to 271 and 751 µm were observed from the light microscope images in Figure 1. A large portion of fine wood fibers with widths of several micrometers was also generated. Wood fibers generated from different ages of trees showed similar morphologies regarding shape and size, with different percentages of wood fibers in various sizes. The light microscope images in Figure 1 showed that wood fibers from trees of L15 and L30 have more fine wood fibers than those from L39. During milling, a significant amount of heat is generated due to the cutting and friction forces, raising the temperatures of the cutting blade, the screen, and the wood particles. The heat softens the wood chips and helps the cutting blade to split the wood fibers from the wood chips, generating long wood fibers. Simultaneously, the heat softens the extractives and resins in the wood, causing extractives, resins, and wood fibers to stick to the cutting blade, screen, and metal wall of the milling chamber. The bonding of extractives and resins to the milling equipment is more severe for milling the wood from the tree of L39 due to the development of heartwood with the extractives and resin content, as demonstrated in the later sections by FTIR and TGA analysis. A noticeable amount of resin and extractive deposits were observed on the cutting blade, screen, and chamber walls when milling the tree of L39. The deposits also made the milling process difficult, with more frequent stops for cleaning. At the same time, wood fibers, especially in fine particle sizes, are lost in the milling process due to the bonding with the resins and extractives sticking with the milling equipment. This phenomenon explains the fewer fine wood fibers identified in Figure 1e for the wood fibers generated from the tree of L39.

The same milling process was applied to the trees exposed to the environment for 6 and 12 months, and wood fibers with different morphologies were generated. The morphologies for the wood fibers generated from trees exposed to the environment for 12 months are shown in Figure 1. The wood fibers with six months of environmental exposure showed a similar trend with those with 12 months of environmental exposure to a less extent, and the images are not shown here. Wood fibers with much more rough surfaces were observed for the L15-12M and L30-12M when compared with L15-0M and L30-0M. Fibrils pulled from the wood fiber surface are shown in the microscopic images for L15-12M and L30-12M, resulting in interconnected wood fiber bundles (Figure 1b and d). Exposure to the environment for 6 and 12 months did change the properties and behaviors of wood during the milling process. The morphologies of wood fiber L39-12M are similar to those of L39-0M, except for a relatively larger portion of smaller fibers which can be observed from the light microscope images. When milling the tree L39 exposed to the environment for 6 and 12 months, resins and extractives were still observed to stick with the milling equipment. However, the larger quantity of the smaller wood fibers shown in Figure 1f indicates that fewer amounts of resin and extractive were in the wood exposed to the environment for 12 months compared with those in zero month of environmental exposure. The tree ages and environmental exposure affected wood fiber morphologies manufactured in this study.

The particle size distributions of the wood fibers generated using the 60-mesh screen during milling were characterized using sieve analysis, and the data are shown in Table 4. All the wood fibers were manufactured using the same equipment with the same operating procedures. Most of the wood fibers

Table 3. Ash content of trees at different exposure times.

	Ash (%)		
ID	0M	6M	12M
L15	0.21 ± 0.02	0.29 ± 0.02	0.32 ± 0.03
L30	0.15 ± 0.01	0.21 ± 0.02	0.30 ± 0.03
L39	0.18 ± 0.02	0.23 ± 0.03	0.37 ± 0.02

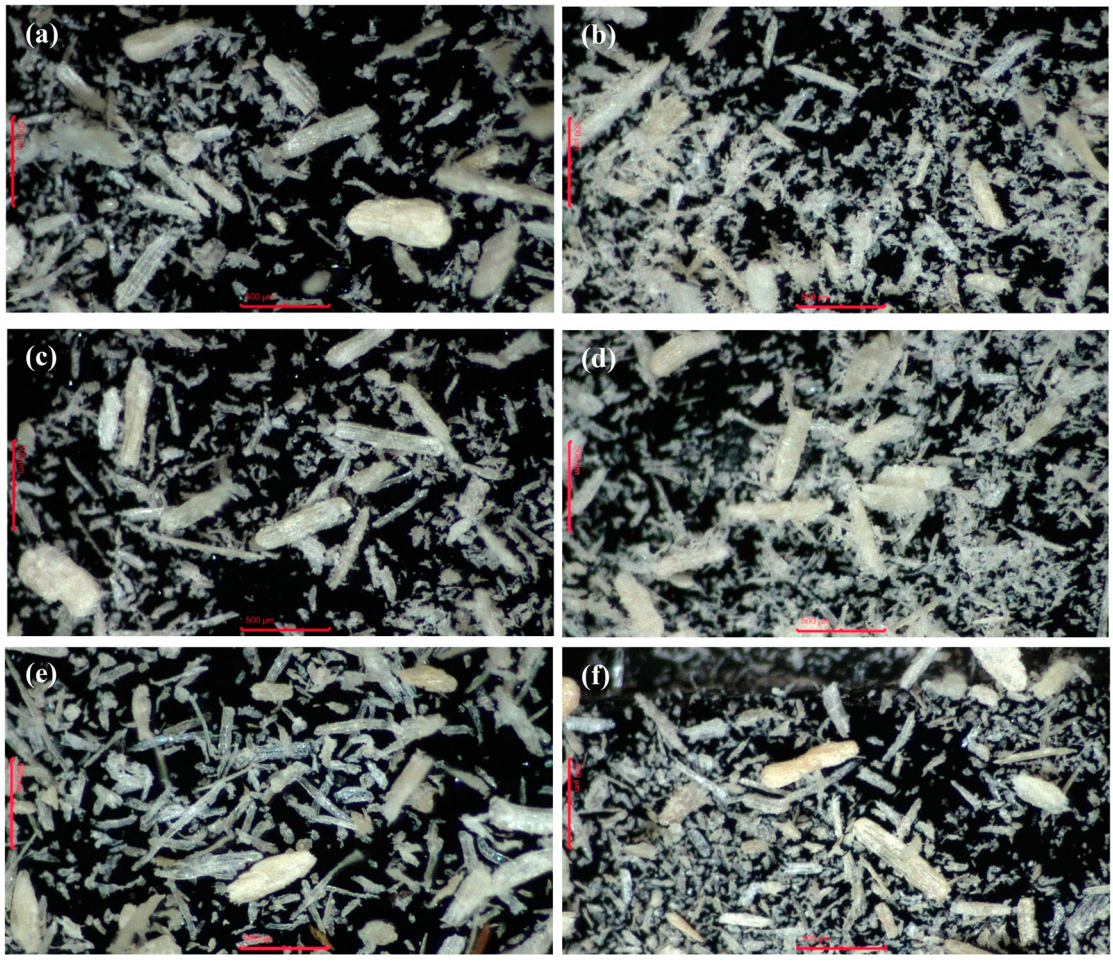

Figure 1. The morphologies of wood fibers from different trees and environmental exposure times (All the scale bars represent 500 μm): (a) L15-0M, (b) L15-12M, (c) L30-0M, (d) L30-12M, (e) L39-0M, and (f) L39-12M.

are smaller than 60 mesh (The test sieve of 60 mesh has a square opening with a side length of 250 μm). Different ages of trees generated wood fibers with different particle size distributions. Wood fibers with particle sizes smaller than 106 μm were collected on the bottom pan and accounted for a significant portion of the wood fibers. The weight percentages of wood fibers smaller than 106 μm for wood collected at 0M are 33.7, 38.5, and 46.5% for L15, L30, and L39, respectively. For the sample collected at 6M, the percentages of these wood fibers (< 106 μm) decreased to 30.6%, 30.7%, and 37.7% for L15, L30, and L39. After the environmental exposure for 12 months, the weight percentages of the same sizes of wood fibers changed to 40.6, 21.9, and 43.6% for L15, L30, and L39. The same environmental exposure of the wood changed the milling behaviors for different ages of trees. However, the factors contributing to the particle size distribution change are not clear. The tree of L30 showed the most significant particle size change after exposure to the natural environment, and the weight percentage of particles with sizes smaller than 106 μm decreased by 43% after 12-month environmental exposure, from 38.5 ± 0.9 for L30-0M to 21.9 ± 2.1 for L30-12M. For the sample of L15, the quantity of particles with sizes smaller than 106 μm increased by 20% with the same environmental exposure time, i.e. the weight percentage of wood fiber particles smaller than 106 μm increased from 33.7 ± 0.6 for L15-0M to 40.6 ± 0.2 for

Table 4. Direct comparison of particle size distributions for the wood fibers.

		Sieve Size (US Standard Mesh)				
ID	Exposure time	60 (425-250 μm)	80 (249-180 μm)	100 (179-150 μm)	140 (149-106 μm)	140 (< 106 μm)
L39	0M	1.5 ± 0.1	13.4 ± 0.6	11.1 ± 0.3	27.5 ± 0.6	46.5 ± 0.7
	6M	3.4 ± 0.1	24.3 ± 0.6	14.3 ± 1.0	20.3 ± 0.7	37.7 ± 0.6
	12M	2.7 ± 0.1	21.2 ± 0.5	11.7 ± 0.1	20.8 ± 0.2	43.6 ± 0.5
L30	0M	2.1 ± 0.3	28.7 ± 0.6	13.6 ± 0.4	17.1 ± 0.2	38.5 ± 0.9
	6M	3.3 ± 0.3	25.7 ± 0.2	16.7 ± 0.1	23.6 ± 0.4	30.7 ± 0.3
	12M	3.7 ± 0.2	28.8 ± 1.1	19.8 ± 0.8	25.8 ± 0.4	21.9 ± 2.1
L15	0M	4.3 ± 0.4	31.1 ± 1.1	13.0 ± 0.7	17.9 ± 0.7	33.7 ± 0.6
	6M	7.5 ± 0.1	30.6 ± 0.3	14.4 ± 0.1	16.9 ± 0.4	30.6 ± 0.2
	12M	3.8 ± 0.1	21.9 ± 0.1	14.0 ± 0.3	19.7 ± 0.0	40.6 ± 0.2

L15-12M. For the sample of L39, this change is from 46.5 ± 0.7 for L39-0M to 43.6 ± 0.5 for L39-12M, only 6% lower. Environmental degradation of downed timber impacted the wood fibers manufacturing process and resulted in different particle size distributions. No specific pattern on wood fiber particle size change was observed. For different ages of trees, the effect of environmental degradation on the obtained wood fiber particle size varied.

Another major difference in particle size distribution is in the particle size ranges of 180–249 µm and 106-149 µm. In the size range of 180 −249 µm, the samples collected at 0M have fiber weight percentages of 31.1, 28.7, and 13.4% for L15, L30, and L39, respectively. The L39 sample has a significantly lower weight percentage compared with the other two. In the size range of 106-149 µm, the opposite is true, i.e. the sample of L39 (27.5 wt.%) has a significantly higher weight percentage of wood fibers than the samples of L15 (17.9 wt.%) and L30 (17.1 wt.%). Manufacturing wood fibers from downed timber of different ages generated different particle size distributions.

Chemical composition change characterization by FT-IR

The wood fibers were characterized using FT-IR, and the spectra of wood fibers from different ages of trees are shown in Figure 2. The peaks in the spectra were assigned based on the literature (Michell 1966, Schultz and Glasser 1986, Collier *et al.* 1992, Pandey and Theagarajan 1997, Pandey 1999, Pandey and Pitman 2003, Traore *et al.* 2018, Aghalari *et al.* 2021) and the band assignments of the 15 peaks are summarized in Table 5. Wood fibers from the three different ages of trees showed similar FT-IR spectra (Figure 2). The only difference is the wood fiber generated from the 39-year-old tree, which has an additional peak at 1694 cm^{-1}. This peak is attributed to the C = O vibration in the carboxylic group in extractive resin acid (Mizzoni and Cesaro 2007, Vahur *et al.* 2011), indicating the development of heartwood for the 39-year-old tree. No such peak is observed for the wood fibers generated from 15 – and 30-year-old trees, and no heartwood is developed.

The chemical composition differences among the different ages of trees were also characterized by calculating the FTIR peak intensity ratios. In this case, the 1509 cm^{-1} peak is treated as a reference for lignin, while according to the literature, the 1731 and 896 cm^{-1} peaks are the hemicellulose and cellulose references, respectively (Pandey and Theagarajan 1997, Rodrigues *et al.* 1998, Pandey and Pitman 2003, Traore *et al.* 2018). A baseline is constructed for measuring the peak areas, represented as the intensity of the peak, and the baseline construction method is shown in Figure 3. The baselines for calculating the areas under the peaks at 1509, 1731, 1159, and 896 cm^{-1} were constructed between 1484 and 1549, 1690 and 1777, 1132 and 1179, and 866 and 919 cm^{-1}, respectively. The ratios of the peak areas for different ages of trees are shown in Table 6. The ratio of I_{1509}/I_{1731} represents the ratio of areas calculated under peak 1509 and 1731cm^{-1} based on the baseline construction shown in Figure 3, which indicates the relative content of lignin to hemicellulose in wood fiber. For the FT-IR spectra of L39, the peak 1694 cm^{-1} partially overlapped with the peak 1731cm^{-1}, and it is hard to calculate the peak area under peak 1731cm^{-1}. Therefore, the I_{1509}/I_{1694} was calculated for the tree of L39-0M, and the data are shown in Table 6. Similarly, the ratio of I_{1509}/I_{896} indicates the relative content of lignin to cellulose in the wood fibers. The ratios of lignin to carbohydrates (I_{1509}/I_{1371} and I_{1509}/I_{1159}) characterized by different functional groups from carbohydrates were also calculated and are shown in Table 6. As the tree grows older, the cellulose content becomes greater (Funda *et al.* 2020), and the ratio of I_{1509}/I_{896} for L39 and L30 is smaller than that of L15. The ratios of lignin to carbohydrates (I_{1509}/I_{1371} and I_{1509}/I_{1159}) are also observed to be smaller for L39 and L30 than that for L15.

After exposure of downed timber to the environment, the chemical compositions of wood fibers produced from downed timber changed. The lignin to hemicellulose ratio (I_{1509}/I_{1731}) statistically increased significantly after 6 – or 12-month environmental exposure for both L15 and L30. The possible faster loss rate of hemicellulose than that of lignin during environmental exposure is the cause. For sample L39, the loss of extractive can be easily observed from the FT-IR spectra in Figure 4. The peak intensity at 1694 cm^{-1}, identifying extractives in L39, decreased dramatically. Simultaneously, extractives are still recognized in the FT-IR spectra in Figure 4 for the L39 wood fibers after 6 and 12 months of environmental exposure. For the L15 and L30, no peaks for extractives are observed. Due to the partial overlap of the extractives and hemicellulose peaks in the FT-IR spectra, the peak ratio of lignin to hemicellulose/extractives is challenging to calculate, and no data are shown in Table 6 for the L39. The lignin to cellulose ratio (I_{1509}/I_{896}) decreased after environmental exposure (Table 6). The lignin component in the wood possibly degraded relatively faster/earlier than the cellulose component in the same environmental exposure process. Two different peak ratios (I_{1509}/I_{11371} and I_{1509}/I_{1159}) characterized the lignin to carbohydrate ratios of the wood fibers after environmental exposure, and these two ratios showed a similar trend of increase. The carbohydrate degraded at a relatively greater speed than the lignin during the same period, mainly dominated by the loss of hemicellulose. This is consistent with the information offered by the ratio change of lignin to hemicellulose (I_{1509}/I_{1731}). No pattern was observed for the chemical composition change between different environmental exposure times for the same tree. The same peak ratio at various environmental exposure times differs, indicating that the three major polymer components in the wood fiber cell wall all have degraded to some extent and behaved differently in each different tree with the same environmental exposure time. The loss of hemicellulose and extractives seem to dominate the process. The complex environmental changes coupled with other impact factors, including impacts of the sun (photodegradation), microorganisms, and insects, make the interpretation of the chemical composition changes challenging.

The sodium hydroxide solubility and EMC

The solubility data in 1% sodium hydroxide (NaOH) solution for the wood fibers are shown in Table 7. Changes in wood fiber chemical compositions, demonstrated by the FT-IR spectra,

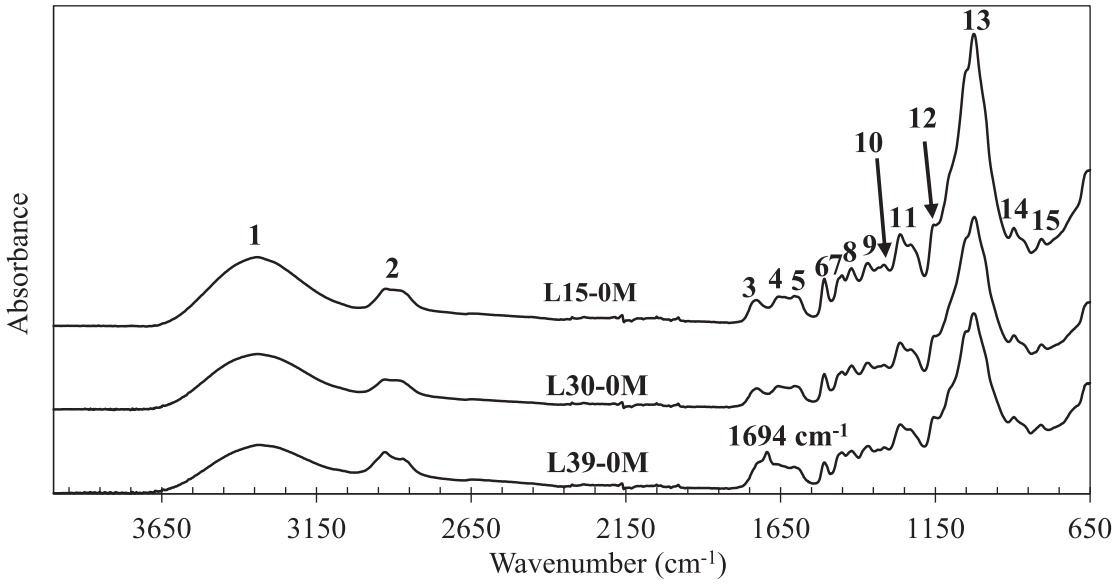

Figure 2. The FT-IR spectra of wood fibers from different ages of trees.

changed the percentages of wood fibers soluble in NaOH solution after environmental exposure. Literature research showed that hemicellulose and lower molecular weight components, including extractives, in the wood cell wall are dissolved in hot alkali solution, and the solubility increases as wood decay progresses (Pandey and Pitman 2003, Villalba *et al.* 2006, Ayrilmis *et al.* 2015). Without environmental exposure, the wood fiber samples of L15 (14.2 ± 0.2 wt.%) and L30 (15.7 ± 0.4 wt.%) have statistically ($F = 353.94$, $p < 0.001$) much lower solubility than that of L39 (22.9 wt.%). These 1% NaOH solubility data are comparable to the data reported in the literature (Broda and Popescu 2019). The wood from the older tree has a higher solubility in a hot alkali solution (Junior and Moreschi 2003, Brand *et al.* 2011).

Table 5. Main FT-IR bands in the wood fibers (Michell 1966, Schultz and Glasser 1986, Collier *et al.* 1992, Pandey and Theagarajan 1997, Pandey 1999, Pandey and Pitman 2003, Traore *et al.* 2018, Aghalari *et al.* 2021).

Peak No.	Wavenumber (cm^{-1})	Band assignments
1	3347	Hydrogen bond stretch
2	2927	C-H stretch
3	1731	Unconjugated C = O in hemicellulose
4	1657	O-H and conjugated C-O in polysaccharides
5	1607	C = O stretch conjugated to aromatic ring, and in carboxylic groups in lignin, carboxylic acid, ester compounds
6	1508	C = C stretch of the aromatic ring in lignin
7	1452	C-H asymmetric deformation in methoxy for lignin and CH_3 and CH_2 in pyran for hemicellulose
8	1421	C-H asymmetric deformation in methoxy, aromatic skeletal vibrations in lignin
9	1371	C-H deformation in cellulose and hemicelluloses
10	1317	CH_2 wagging in crystalline cellulose
11	1264	C-O vibration in guaiacyl rings
12	1159	C-O-C asymmetric stretch in cellulose and hemicellulose
13	1026	C-O stretching in primary alcohols in cellulose
14	896	C-H deformation of beta-glycosidic linkages in cellulose
15	808	Vibration of mannan in hemicellulose and C-H out of plane bending in phenyl rings

After six months of exposure to the natural environment, the solubility of L15-6M increased marginally from 14.2 ± 0.2 (L15-0M) to 15.3 ± 0.5 wt.%, and the L30-6M remained the same when compared to L30-0M. The solubility of L39-6M decreased from 22.9 ± 0.6 to 17.7 ± 0.7 wt.% (i.e. 22.7%). After 12 months of environmental exposure, the solubility values of the samples L15, L30, and L39 were 12.4 ± 1.0, 11.1 ± 0.5, and 21.2 ± 0.5 wt.%, respectively. The samples of L15 ($F = 15.46$, $p = 0.004$) and L30 ($F = 46.92$, $p < 0.001$) after 12 months of environmental exposure have statistically significantly lower soluble components than those with zero and six months of environmental exposure. Conversely, the sample L39 ($F = 185.32$, $p < 0.001$) with 12 months of environmental exposure has a higher soluble portion than six months, slightly lower than zero months. Literature showed that the degradation of wood in the natural environment generated a higher fraction of low molecular weight cell wall components, resulting in an increased solubility in NaOH (Kawase 1962). However, the experimental data showed almost no change in solubility data with six months of environmental exposure and decreased solubility with 12 months of exposure for the tree of L15 and L30. A reasonable explanation is that the wood samples lost a small portion of hemicellulose, and low molecular weight components generated by degradation during the environmental exposure for six months, probably washed away by the rain or transformed into volatiles to the environment. The loss of these wood components led to the mass reduction of the wood sample and degraded products, resulting in a minor solubility change within six months of environmental exposure. The minor mass loss can also be demonstrated by the minor wood density change shown in Table 2. With the 12 months of environmental exposure, the NaOH solubility significantly decreased. The loss of the degraded wood components probably dominated the environmental degradation process in the period, leading to a considerable decrease in NaOH solubility. This phenomenon of significant mass reduction can also be explained by the significant drop in the

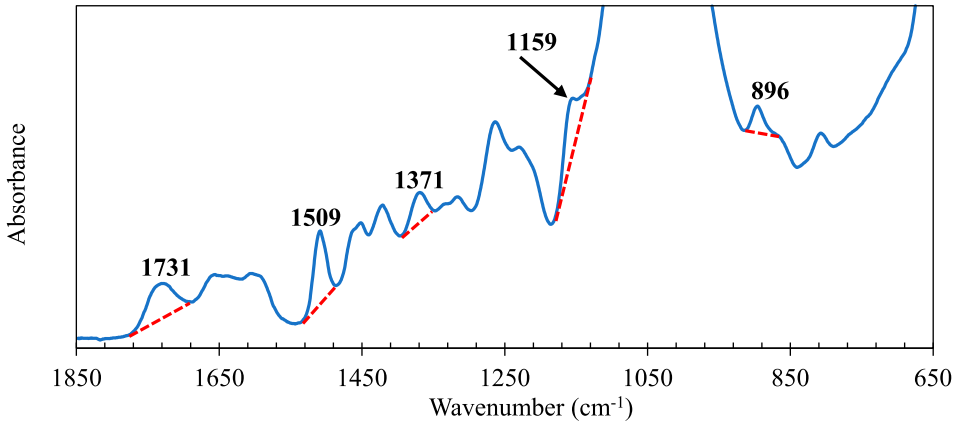

Figure 3. Measurement of peak area for characterizing the chemical composition of wood fibers.

wood density shown in Table 2 for this period of environmental exposure. For the wood sample of L39, a significant decrease in the NaOH solubility with six months of environmental exposure is mainly caused by the dominant loss of extractives stored in the heartwood of the sample during the environmental degradation process, which is soluble in the 1% NaOH solution. The loss of the extractive can be confirmed by the decreased FT-IR peak for extractives (1694 cm^{-1} peak in Figure 4), which decreased significantly. Minimum wood degradation occurred in this period since the extractives helped to protect the wood from degradation (Kirker *et al.* 2013). With continuous exposure to the environment for another six months, the NaOH solubility increased with degradation, and the solubility increased to 21.2 ± 0.5 wt.%. Within this period, the extractive loss is not significant, as demonstrated by the minimum extractive peak change in the FT-IR spectra in Figure 4. The increased NaOH solubility also indicates that the loss of degraded components to the environment in this period is minor for the L39 sample, which can also explain the insignificant wood density change shown in Table 2 for L39 in this period. The residual extractives in the wood may help prevent the loss of environmentally degraded wood products.

The EMC values of the generated wood fibers at 35 °C and different RH levels are shown in Table 8. The EMC of wood reflects the change in hygroscopicity of the wood, which is the function of chemical composition (Choong 1969), depending on RH and temperature. At 35 °C, the EMC values for all the wood fibers increased with increasing RH levels. The values of EMC in this experiment are comparable to those reported in the literature (Choong 1969, Glass *et al.* 2018). At 35% RH, the EMC values of all the samples were between 4.27 - 4.94%. The EMC gradually increased to 18.1 - 20.1% at 90% RH. At all RH levels, the EMC values of wood fibers from the tree of L39 were significantly lower than those of L15 and L30. The significantly lower EMC values of L39, when compared to L15 and L30, can be related to the tree's age and extractive content because older trees are less hygroscopic due to higher extractive content. The environmental exposure of six months changed the EMC values for the wood fibers. For different RH levels, the environmental exposure effect differs. For samples of L15 and L30, the EMC increased by a maximum of approximately 4% (EMC value changed from 4.76 wt.% for L30-0M to 4.94 wt.% for L30-6M at 35% RH). The complex degradation of wood fibers with exposure to the natural environment, including the degradation of hemicellulose, lignin, and cellulose, resulted in complex moisture absorption behavior changes. For the sample of L39, the EMC values increased in the range from 7 to 10% after six months of environmental exposure. This is potentially associated with the removal of extractives during environmental exposure, resulting in increased hygroscopicity which can absorb more moisture. The effect of the loss of extractives probably dominated the process for the L39 wood fibers for moisture absorption properties. Our observation of an increase in EMC aligns with the study (Musah *et al.* 2022) for 6M samples. Another six months of environmental exposure decreased moisture absorption, leading to lower EMC values,

Table 6. FTIR spectrum peak area ratios for wood fibers from different ages of trees with varying environmental exposure times.

		Relative intensities of lignin against typical peaks for carbohydrates			
Sample	Exposure	I_{1509}/I_{1731}	I_{1509}/I_{896}	I_{1509}/I_{1371}	I_{1509}/I_{1159}
	0M	0.75 ± 0.01	4.74 ± 0.92	2.55 ± 0.15	1.56 ± 0.11
L15	6M	1.01 ± 0.08	3.25 ± 0.12	2.89 ± 0.33	1.51 ± 0.05
	12M	1.30 ± 0.09	2.47 ± 0.11	2.60 ± 0.13	1.38 ± 0.11
	0M	0.70 ± 0.06	3.83 ± 0.52	2.05 ± 0.16	1.26 ± 0.04
L30	6M	1.10 ± 0.04	2.84 ± 0.07	2.42 ± 0.23	1.33 ± 0.12
	12M	1.06 ± 0.05	2.63 ± 0.21	2.49 ± 0.11	1.43 ± 0.03
	0M	3.96 ± 1.08*	3.90 ± 0.58	1.83 ± 0.02	1.26 ± 0.04
L39	6M	–	2.52 ± 0.22	2.26 ± 0.19	1.39 ± 0.11
	12M	–	2.92 ± 0.23	2.21 ± 0.09	1.46 ± 0.22

*denote the ratio of I_{1509}/I_{1694}.

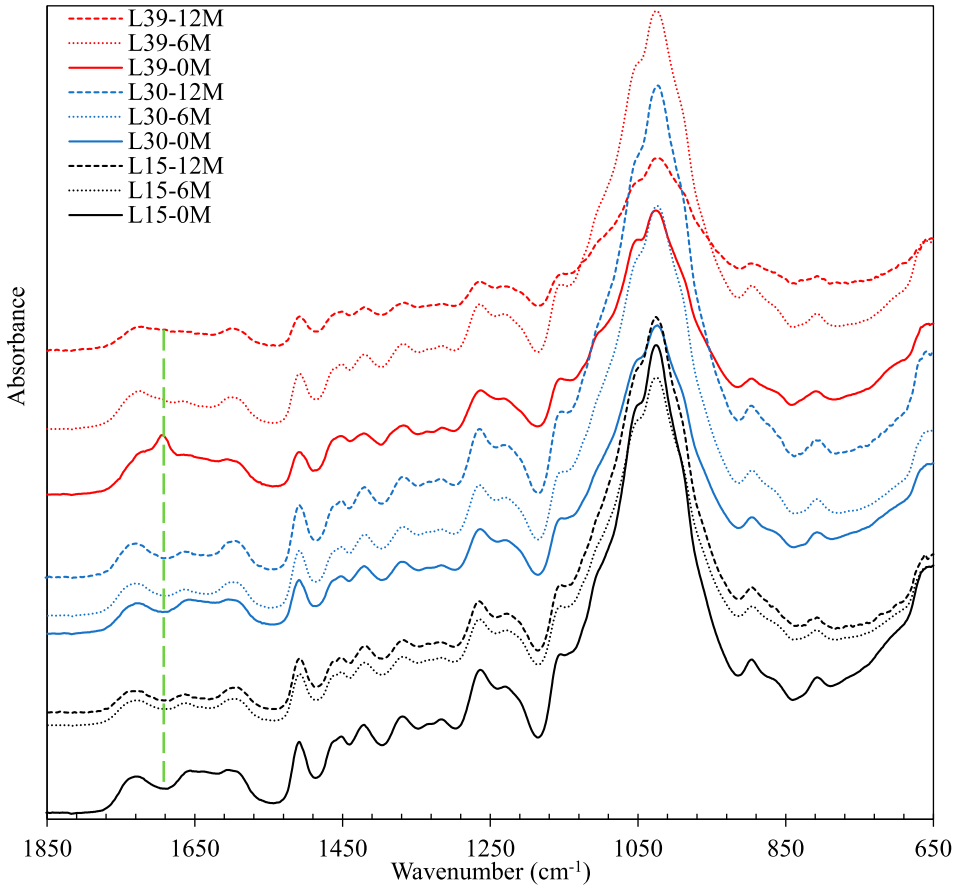

Figure 4. The FT-IR spectra of wood fibers with different environmental exposure times.

as demonstrated in Table 8. The moisture absorption behavior for this period due to further wood degradation is difficult to interpret.

The thermal properties

TGA was used to determine the thermal properties of the wood fibers generated from downed timber. A typical TGA thermogram of the wood fibers is shown in Figure 5a for the sample of L39-0M. The first (DTG) and second derivatives of the thermogram to temperature are also included. The TGA thermogram shows the function of the mass of the wood fibers versus temperature at the temperature ramping rate of 10 °C/minute. The first derivative of the thermogram describes the mass loss rate that occurred at a specific temperature. The second derivative helps to determine how fast the mass loss rate changes at a temperature. From the TGA and DTG thermograms, it is difficult to consistently identify the maximum thermal degradation rates (i.e. mass loss rates) for the primary wood fiber cell wall components, including hemicellulose and lignin, due to the overlap of their DTG peaks with that of cellulose. This research used the second derivative curve to determine the maximum degradation rates for the primary chemical components in the wood fibers to evaluate the effect of age and environmental exposure on the thermal properties (Grønli *et al.* 2002).

When the temperature of wood fiber increased, wood fibers initially lost moisture, and the moisture evaporation rate increased with increasing temperature. The maximum moisture loss rate occurred at around 70 °C, where the second derivative changed from positive to negative values at this inflection point (Figure 5a). The mass loss rate due to moisture evaporation reached the maximum value when the change of water evaporation rate approached zero. As the temperature continued to increase, another inflection point was reached for the second derivative curve, and the DTG value also approached approximately zero (Figure 5a). The moisture loss phase ends for the wood fibers at this point. The initial moisture loss was observed in all the wood fibers, with a mass change of approximately 8 wt.% at 138 °C for the L39-0M sample (Figure 5a). The maximum moisture evaporation rate occurred at the same temperature (70 ± 1 °C) for the samples of L15-0M and L30-0M. However, the moisture loss stage finished at a different temperature for L15-0M and L30-0M (around 150 ± 1 °C) than L39-0M (138 ± 1 °C). This moisture loss stage ending point is defined as the inflection point of the second derivative curve. For sample L39, the extractives probably started degrading at

Table 7. Sodium hydroxide (1%) solubility of different trees at different exposure times.

	Solubility (wt. %)		
Sample	0M	6M	12M
L15	14.2 ± 0.2	15.3 ± 0.5	12.4 ± 1.0
L30	15.7 ± 0.4	15.7 ± 1.0	11.1 ± 0.5
L39	22.9 ± 0.6	17.7 ± 0.7	21.2 ± 0.5

Table 8. The EMC values the wood fibers at different RH levels.

Sample	Exposure time	EMC (wt. %)				
		35% RH	45% RH	60% RH	75% RH	90% RH
L15	0M	4.77 ± 0.14	6.37 ± 0.01	9.02 ± 0.02	12.8 ± 0.03	19.4 ± 0.05
	6M	4.85 ± 0.01	6.41 ± 0.04	9.21 ± 0.02	13.1 ± 0.05	19.5 ± 0.05
	12M	4.62 ± 0.01	6.16 ± 0.01	8.87 ± 0.01	12.6 ± 0.05	18.9 ± 0.18
L30	0M	4.76 ± 0.04	6.35 ± 0.04	9.07 ± 0.09	12.9 ± 0.04	19.6 ± 0.09
	6M	4.94 ± 0.01	6.50 ± 0.09	9.40 ± 0.02	12.9 ± 0.09	20.1 ± 0.14
	12M	4.66 ± 0.01	6.22 ± 0.01	8.94 ± 0.11	13.4 ± 0.08	19.4 ± 0.12
L39	0M	4.39 ± 0.02	5.81 ± 0.03	8.34 ± 0.07	12.0 ± 0.12	18.1 ± 0.03
	6M	4.83 ± 0.06	6.36 ± 0.10	9.14 ± 0.12	12.8 ± 0.38	19.6 ± 0.24
	12M	4.27 ± 0.01	5.73 ± 0.01	8.35 ± 0.01	12.0 ± 0.26	18.7 ± 0.11

138 °C, which was represented by an increasing rate of the mass loss rate change in the second derivative curve. For L15-0M and L39-0M, the second derivative value increased as the hemicellulose component started to degrade at around 150 °C, as demonstrated by the different values of the second derivate curves in Figure 5b.

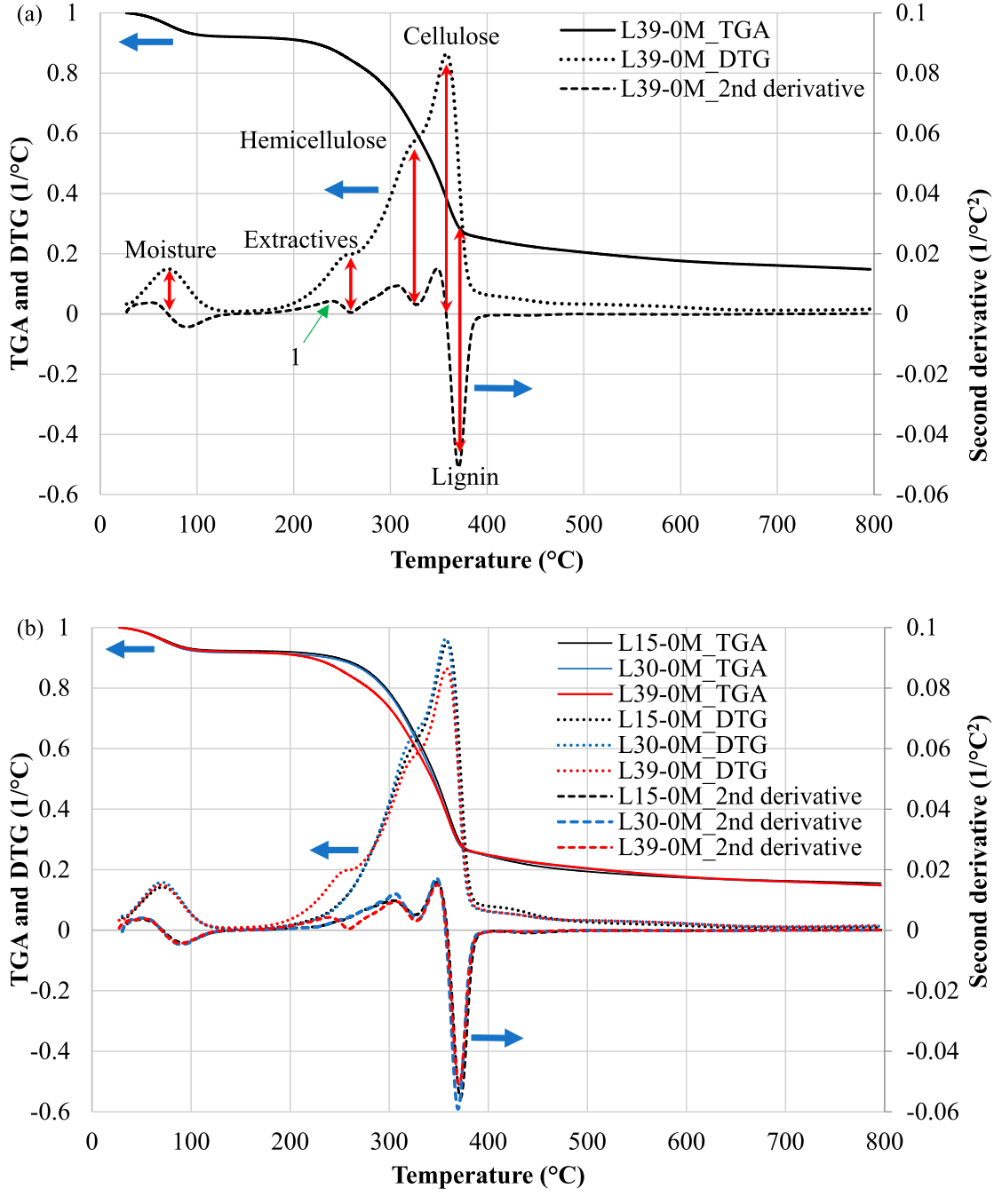

Figure 5. The thermal properties of the wood fibers showing the analysis method (a) and the comparison among L15-0M, L30-0M, and L39-0M (b).

Table 9. The thermal degradation peak temperatures of the primary chemical components of the wood fibers.

Sample	Exposure time	Thermal degradation peak temperature (°C)				
		Moisture	Extractives	Hemicellulose	Cellulose	Lignin
L15	0M	70 ± 1	–	326 ± 1	357 ± 2	370 ± 2
	6M	70 ± 1	–	323 ± 3	352 ± 1	365 ± 1
	12M	68 ± 1	–	327 ± 1	352 ± 1	366 ± 1
L30	0M	70 ± 1	–	327 ± 1	354 ± 2	367 ± 3
	6M	70 ± 1	–	323 ± 2	354 ± 1	365 ± 1
	12M	68 ± 2	–	326 ± 1	352 ± 1	365 ± 1
L39	0M	70 ± 1	259 ± 1	327 ± 1	358 ± 1	371 ± 1
	6M	72 ± 1	252 ± 1	327 ± 1	360 ± 1	372 ± 2
	12M	72 ± 2	252 ± 1	327 ± 1	351 ± 2	365 ± 2

As the temperature increased further, extractives and hemicellulose in the sample of L39-0M thermally degraded simultaneously, and the second derivative value kept growing, i.e. the slope of the mass loss rate (DTG) curve kept increasing. At the temperature where peak #1 is shown in Figure 5a, the slope of the mass loss rate curve reached a maximum, followed by a lower slope of the mass loss rate curve. During this period, both mass loss rates of extractives and hemicellulose accelerated with increasing temperature. Then the rate of change of the mass loss rate decreased as the extractive degraded, and a minimum point approached as the mass loss rate due to the extractive thermal degradation maximized. The temperature of the extractive thermal degradation peak is identified as 259 °C for L39-0M (red arrow in Figure 5a for extractives). For L15-0M and L30-0M, no such peak for extractives was observed (Figure 5b). The difference can also be observed in the TGA and DTG thermograms.

Similarly, the thermal degradation peaks for hemicellulose (327 ± 1 °C), cellulose (358 ± 1 °C), and lignin (371 ± 1 °C) were identified for L39-0M, as shown in Figure 5a and Table 9. The thermal degradation peak of cellulose was identified when the second derivative changed the sign from positive to negative. The thermal degradation process of cellulose overlapped with those of hemicellulose and lignin, and the thermal degradation of cellulose dominated the process within this temperature range. After reaching the greatest slope for the mass loss rate curve of cellulose (DTG curve), the slope of the mass loss rate decreased. Simultaneously, the slope of the DTG curve for hemicellulose also decreased while the slope of the DTG curve for lignin increased. With the dominance of the thermal degradation of cellulose, the degradation peak was reached when the slope of the DTG curve decreased to zero. No significant difference in the thermal degradation peak temperatures was observed for the primary chemical components of three samples of L15-0M, L30-0M, and L39-0M, including hemicellulose, cellulose, and lignin (Figure 5b and Table 8).

The thermal degradation peak temperatures of the three major chemical components of wood fibers are summarized in Table 8. The temperatures of the maximum moisture evaporation rate for wood fibers are also included, and no significant difference was observed for different environmental exposure periods. For the sample of L39, the thermal degradation peak temperature for the extractives decreased from 259 ± 1 °C to 252 ± 1 °C after six months of environmental exposure. The main reason is the loss of extractives during natural environmental exposure, demonstrated by FT-IR spectra and NaOH

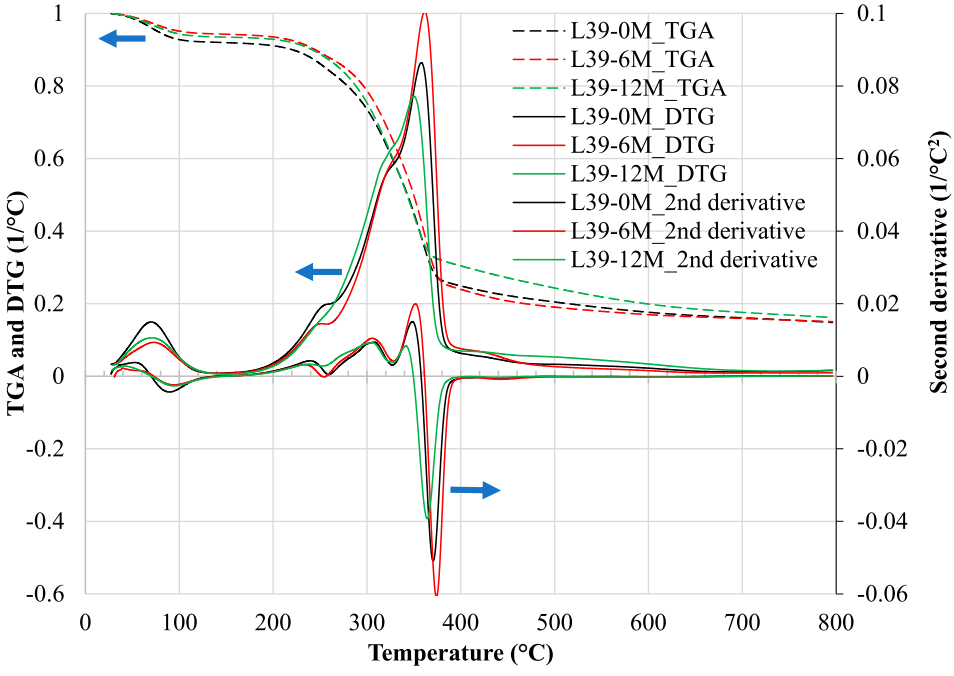

Figure 6. The thermal properties of sample L39 with different environmental exposure periods.

solubility changes. An additional six months of exposure did not change the extractive thermal degradation peak temperature, matching the FT-IR and NaOH solubility study observations. The loss of extractives can also be easily identified in the TGA and DTG thermograms for the sample of L39 in Figure 6. The thermal degradation peak temperatures of hemicellulose for all the wood fibers did not change significantly. The slight value variation may indicate the hemicellulose loss during environmental degradation did not dramatically impact the thermal stability of the hemicellulose component in wood fibers.

For the wood fibers of L39, the environmental degradation in the first six months mainly resulted in a significant extractive loss and negligible thermal degradation peak temperature change for cellulose and lignin (Table 9). When the sample of L39 was exposed to the natural environment for another six months, the thermal degradation peak temperatures for cellulose and lignin decreased from 360 ± 1 and 372 ± 2 to 351 ± 2 and 365 ± 2, respectively (Figure 6 and Table 9). These changes can also be easily identified in the TGA and DTG curves. Loss of extractives in the first six months accelerated the environmental degradation of cellulose and lignin in the second six months. This is consistent with the literature study that extractives can protect wood from environmental degradation (Kirker *et al.* 2013). During the second six-month period, the degraded products of wood were still stored in the wood fibers, as demonstrated by the density and 1% NaOH solubility data. The degraded wood products are small molecules that resulted in lower thermal degradation temperature. No significant effect on the thermal degradation peak temperatures was observed for the samples of L15 and L30 on cellulose and lignin. However, the main change seems to appear in the initial six months of environmental exposure for L15 and L30 (Table 9). The variations in the thermal degradation peak temperatures may indicate a complex environmental effect on the degradation of cellulose and lignin components in L15 and L30. Loss of the degraded products to the environment from cellulose and lignin is the primary cause of no thermal behavior changes in the second environmental exposure period. The significant density changes in this exposure period for L15 and L30 shown in Table 2 confirm this explanation.

Conclusions

In this study, loblolly pine trees at the age of 15-, 30-, and 39-year-old were selectively felled and exposed to the local natural environment. Log samples were collected at six-month intervals within one year. The wood fibers from these samples were then characterized based on physical, morphological, chemical, and thermal properties to understand the effect of environmental exposure. The densities of the wood sample were also examined.

The wood fibers generated from different ages of trees using the same milling process showed different particle size distributions. The particle size distribution was characterized using sieve analysis. Older trees have a smaller portion of particles in the size range of 180–249 μm, and a much larger portion of particles in the size range smaller than 149 μm. Different ages of trees behaved differently with the same mechanical size reduction procedure. The wood fibers produced from the 39-year-old tree (L39) have developed heartwood with a significant amount of extractives. The extractives were deposited on the milling machine walls, impacting the milling process for the 39-year-old log sample. The wood fibers of L39 (22.9 ± 0.6 wt.%) also have a much higher 1% NaOH solubility than the wood fibers of L15 (14.2 ± 0.2 wt.%) and L30 (15.7 ± 0.4 wt.%) due to the extractives. Simultaneously, the extractives in the L39 sample make the wood fibers absorb slightly less moisture than the other two samples at the same temperature and RH. The extractives in the L39 sample did not change the primary chemical component thermal degradation peak temperatures when compared with those of L15 and L30 samples.

Environmental exposure did change the properties of the wood fibers generated from downed timber. The three primary chemical components of wood fibers, including hemicellulose, cellulose, and lignin, were degraded to some extent with complex causes. Significant density changes were observed after 12 months of environmental exposure caused by the loss of degraded wood components for L15 and L30. No such change occurred in the first six months of environmental exposure. Loss of extractives in L39 was observed in the first six months of environmental exposure, and no significant density change was observed for the L39 sample within the one-year research period. The residual extractives in L39 may help minimize the loss of degraded products from wood during environmental exposure, as demonstrated by minor wood density change and the increased 1% NaOH solubility. Environmental exposure also changed the wood fiber's morphological properties. Rough surfaces were created on wood fibers, which could positively impact the utilization of these wood fibers for manufacturing wood polymer composites. Environmental exposure of 12 months did not significantly change the thermal behaviors of the L15 and L30 samples. This could be related to the loss of the degraded wood products from the three major chemical components of wood, with the undegraded part having the same thermal behaviors as the original wood. The environmental degradation of the L39 sample after the first phase of losing extractives in the first six months of environmental exposure caused the thermal degradation peak temperature changes for cellulose and lignin for up to 9 and 6 °C, respectively. The thermal degradation peak shifting could be the representative effect of the residues of degraded wood components which are still stored in the wood fibers, probably caused by the extractives left in the wood. This magnitude of temperature changes in the thermal stability of wood fibers would not pose any concerns about using wood fibers from downed timber in manufacturing wood polymer composites using polyolefin-based polymer systems. Future work will investigate the wood polymer composites manufactured using these wood fibers generated from downed timber. The mechanical properties of wood polymer composites impacted by the wood fibers with other various characteristics will be evaluated.

Data availability statement

The data that support the findings of this study are available from the corresponding author, [YP], upon reasonable request.

Disclosure statement

No potential conflict of interest was reported by the author(s).

Funding

This work was supported by the [USDA Forest Service Southern Research Station Downed Timber Research Program] under Grant [G00013505]; [Alabama Agricultural Experiment Station and the Hatch program of the National Institute of Food and Agriculture, U.S. Department of Agriculture] under Grant [ALA031-1-19091]; and [USDA National Institute of Food and Agriculture, McIntire Stennis project] under Grant [ALAZ 00079].

References

Aghalari, A., et al., 2021. A bilevel model formulation for solving a post-hurricane damaged timber management problem. *Computers & Industrial Engineering*, 162, doi:10.1016/j.cie.2021.107726.

Ayrilmis, N., Kaymakci, A., and Gulec, T., 2015. Potential use of decayed wood in production of wood plastic composite. *Industrial Crops and Products*, 74, 279–284. doi:10.1016/j.indcrop.2015.04.024.

Blanchette, R.A., et al., 1997. Cell wall alterations in loblolly pine wood decayed by the white-rot fungus, ceriporiopsis subvermispora. *Journal of Biotechnology*, 53, 203–213. doi:10.1016/S0168-1656(97)01674-X.

Brand, M.A., et al., 2011. Storage as a tool to improve wood fuel quality. *Biomass and Bioenergy*, 35, 2581–2588. doi:10.1016/j.biombioe.2011.02.005.

Broda, M., and Popescu, C.M., 2019. Natural decay of archaeological oak wood versus artificial degradation processes — An FT-IR spectroscopy and X-ray diffraction study. *Spectrochimica Acta Part A: Molecular and Biomolecular Spectroscopy*, 209, 280–287. doi:10.1016/j.saa.2018.10.057.

Choong, E., 1969. Effect Of extractives on shrinkage and other hygroscopic properties of ten southern pine woods. *Wood and Fiber Science*, 1, 124–133.

Collier, W.E., Schultz, T.P., and Kalasinsky, V.F., 1992. Infrared study of lignin: reexamination of aryl-alkyl ether C—O stretching peak assignments. *Holzforschung*, 46, 523–528. doi:10.1515/hfsg.1992.46.6.523.

Curling, S.F., Clausen, C.A., and Winandy, J.E., 2001. The effect of hemicellulose degradation on the mechanical properties of wood during brown rot decay. Nara, Japan: The International Research Group on Wood Preservation.

Curling, S.F., Clausen, C.A., and Winandy, J.E., 2002. Relationships between mechanical properties, weight loss, and chemical composition of wood during incipient brown-rot decay. *Forest Prod J*, 52, 34–39.

Eastwood, D.C., 2014. ACS symposium series. *Acs Sym Ser*, 1158, 93–112. doi:10.1021/bk-2014-1158.ch005.

Elsheikh, A.H., et al., 2022. Recent progresses in wood-plastic composites: Pre-processing treatments, manufacturing techniques, recyclability and eco-friendly assessment. *Cleaner Engineering and Technology*, 8, doi:10.1016/j.clet.2022.100450.

Funda, T., et al., 2020. Predicting the chemical composition of juvenile and mature woods in Scots pine (pinus sylvestris L.) using FTIR spectroscopy. *Wood Science and Technology*, 54, 289–311. doi:10.1007/s00226-020-01159-4.

Glass, S.V., et al., 2018. Quantifying and reducing errors in equilibrium moisture content measurements with dynamic vapor sorption (DVS) experiments. *Wood Science and Technology*, 52, 909–927. doi:10.1007/s00226-018-1007-0.

Grønli, M.G., Varhegyi, G., and Di Blasi, C., 2002. Thermogravimetric analysis and devolatilization kinetics of wood. *Industrial & Engineering Chemistry Research*, 41, 4201–4208. doi:10.1021/ie0201157.

Groom, L., Mott, L., and Shaler, S., 2002a. Mechanical properties of individual southern pine fibers. Part I. Determination and Variability of Stress-Strain Curves with Respect to Tree Height and Juvenility. *Wood and Fiber Science*, 34, 14–27.

Groom, L., Shaler, S., and Mott, L., 2002b. Mechanical properties of individual southern pine fibers. part III: global relationships between fiber properties and fiber location within an individual tree. *Wood and Fiber Science*, 34, 238–250.

Hastrup, A.C.S., et al., 2012. Differences in crystalline cellulose modification due to degradation by brown and white rot fungi. *Fungal Biology*, 116, 1052–1063. doi:10.1016/j.funbio.2012.07.009.

Hehar, G., et al., 2014. Ignition and volatilization behavior of dust from loblolly pine wood. *Fuel Processing Technology*, 127, 117–123. doi:10.1016/j.fuproc.2014.04.036.

Junior, G.B., and Moreschi, J.C., 2003. Physical-mechanical properties and chemical composition of pinus taeda mature wood following a forest fire. *Bioresource Technology*, 87, 231–238. doi:10.1016/S0960-8524(02)00242-0.

Kawase, K., 1962. Chemical components of wood decayed under natural condition and their properties. *Journal of the Faculty of Agriculture*, 52, 186–245.

Kirker, G.T., et al., 2013. The role of extractives in naturally durable wood species. *International Biodeterioration & Biodegradation*, 82, 53–58. doi:10.1016/j.ibiod.2013.03.007.

Knoll, C.S., Wong, B.M., and Roy, D.N., 1993. The chemistry of decayed aspen wood and perspectives on Its utilization. *Wood Science and Technology*, 27, 439–448. doi:10.1007/BF00193867.

Kupfer, J.A., et al., 2008. Patterns of forest damage in a southern Mississippi landscape caused by hurricane katrina. *Ecosystems*, 11, 45–60. doi:10.1007/s10021-007-9106-z.

Lindenmayer, D.B., Burton, P.J., and Franklin, J.F., 2008. *Salvage logging and its ecological consequences*. Washington, DC: Island Press.

Long, A., et al., 2005. Assessment and management of hurricane damaged timberland: SS-FOR 22/FR154, 1/2005.EDIS, 2005, doi:10.32473/edis-fr154-2005.

McMillin, C.W., 1968a. Ash content of loblolly pine wood as related to specific gravity, growth rate, and distance from pith. *Wood Science*, 2, 26–30.

Mcmillin, C.W., 1968. Morphological characteristics of loblolly pine wood as related to specific gravity growth rate and distance from pith. *Wood Science and Technology*, 2, 166.

Michell, A.J., 1966. Infrared spectra of lignin model compounds and of lignins from eucalyptus regnans. *Australian Journal of Chemistry*, 19, 2285. doi:10.1071/CH9662285.

Mitchell, D., Smidt, M., and Mcdonald, T., 2021. Issues and opportunities for salvaging storm damaged wood. *NE*, 2692–2698. doi:10.13031/aim.202101231.

Mizzoni, F., and Cesaro, S.N., 2007. Study of the organic residue from a 2600-year old etruscan plumpekanne. *Spectrochimica Acta Part A: Molecular and Biomolecular Spectroscopy*, 68, 377–381. doi:10.1016/j.saa.2006.12.005.

Mott, L., Groom, L., and Shaler, S., 2002. Mechanical properties of individual southern pine fibers. Part II. Comparison of Earlywood and Latewood Fibers with Respect to Tree Height and Juvenility. *Wood and Fiber Science*, 34, 221–237.

Musah, M., et al., 2022. Field assessment of downed timber strength deterioration rate and wood quality using acoustic technologies. *Forests*, 13, doi:10.3390/f13050752.

Oyedeji, O., et al., 2016. The effect of storage time and moisture content on grindability of loblolly pine (pinus taeda L.). *European Journal of Wood and Wood Products*, 74, 857–866. doi:10.1007/s00107-016-1070-x.

Pandey, K.K., 1999. A study of chemical structure of soft and hardwood and wood polymers by FTIR spectroscopy. *Journal of Applied Polymer Science*, 71, 1969–1975. doi:10.1002/(Sici)1097-4628(19990321)71:12<1969::Aid-App6>3.3.Co;2-4.

Pandey, K.K., and Pitman, A.J., 2003. FTIR studies of the changes in wood chemistry following decay by brown-rot and white-rot fungi. *International Biodeterioration & Biodegradation*, 52, 151–160. doi:10.1016/S0964-8305(03)00052-0.

Pandey, K.K., and Theagarajan, K.S., 1997. Analysis of wood surfaces and ground wood by diffuse reflectance (DRIFT) and photoacoustic (PAS)

Fourier transform infrared spectroscopic techniques. *Holz als Roh- und Werkstoff*, 55, 383–390. doi:10.1007/s001070050251.

Peng, Y.C., Han, Y.S., and Gardner, D.J., 2012. Spray-Drying cellulose nanofibrils: effect of drying process parameters on particle morphology and size distribution. *Wood and Fiber Science*, 44, 448–461.

Prestemon, J.P., and Holmes, T.P., 2004. Market dynamics and optimal timber salvage after a natural catastrophe. *Forest Sci*, 50, 495–511.

Prestemon, J.P., and Holmes, T.P., 2010. Economic impacts of hurricanes on forest owners vol 2. General Technical Report PNW-GTR-802.

Radtke, P.J., et al., 2004. A proposed model for deadwood C production and decay in loblolly pine plantations. *Environmental Management*, 33, S56–S64. doi:10.1007/s00267-003-9117-2.

Rodrigues, J., Faix, O., and Pereira, H., 1998. Determination of lignin content of *eucalyptus globulus* wood using FTIR spectroscopy. *Holzforschung*, 52, 46–50. doi:10.1515/hfsg.1998.52.1.46.

Rutledge, B.T., et al., 2021. Tree, stand, and landscape factors contributing to hurricane damage in a coastal plain forest: post-hurricane assessment in a longleaf pine landscape. *Forest Ecology and Management*, 481, doi:10.1016/j.foreco.2020.118724.

Schultz, T.P., and Glasser, W.G., 1986. Proposed mechanism for the nitrobenzene oxidation of lignin. *Holzforschung*, 40, 93–97.

Stanturf, J.A., Goodrick, S.L., and Outcalt, K.W., 2007. Disturbance and coastal forests: A strategic approach to forest management in hurricane impact zones. *Forest Ecology and Management*, 250, 119–135. doi:10.1016/j.foreco.2007.03.015.

Traore, M., Kaal, J., and Cortizas, A.M., 2018. Differentiation between pine woods according to species and growing location using FTIR-ATR. *Wood Science and Technology*, 52, 487–504. doi:10.1007/s00226-017-0967-9.

Vahur, S., Kriiska, A., and Leito, I., 2011. Investigation of the adhesive residue on the flint insert and the adhesive lump found from the pulli early mesolithic settlement site (Estonia) by micro-Atr-Ft-Ir spectroscopy. *Estonian Journal of Archaeology*, 15, 3–17. doi:10.3176/arch.2011.1.01.

Via, B.K., et al., 2006. Variation of kink and curl of longleaf pine (pinus palustris) fibers. *Characterization of the Cellulosic Cell Wall*, 180–191. doi:10.1002/9780470999714.ch14.

Via, B.K., et al., 2007. Within tree variation of lignin, extractives, and microfibril angle coupled with the theoretical and near infrared modeling of microfibril angle. *IAWA Journal*, 28, 189–210. doi:10.1163/22941932-90001633.

Via, B.K., et al., 2009. Mechanical response of longleaf pine to variation in microfibril angle, chemistry associated wavelengths, density, and radial position. *Composites Part A: Applied Science and Manufacturing*, 40, 60–66. doi:10.1016/j.compositesa.2008.10.007.

Villalba, L.L., Scott, G.M., and Schroeder, L.R., 2006. Modification of loblolly pine chips with Ceriporiopsis subvermispora part 1: Effect of fungal treatment. *Journal of Wood Chemistry and Technology*, 26, 339–348. doi:10.1080/02773810601105177.

Vogt, J.T., et al., 2020. Interactions between weather-related disturbance and forest insects and diseases in the southern United States. Gen. Tech. Rep. SRS–255, Asheville, NC: U.S. Department of Agriculture Forest Service, Southern Research Station. doi:10.2737/SRS-GTR-255.

Wong, A.H.H., and Wilkes, J., 1988. Progressive changes in cell wall components of pinus radiata during decay. *International Biodeterioration*, 24, 481–487. doi:10.1016/0265-3036(88)90036-X.

Yao, Q., et al., 2022. Nature versus humans in coastal environmental change: assessing the impacts of hurricanes zeta and Ida in the context of beach nourishment projects in the Mississippi river delta. *Remote Sensing*, 14, doi:10.3390/rs14112598.

Yeh, T., 2006. *Chemical and structural characterizations of juvenile wood, mature wood, and compression wood of loblolly pine (pinus taeda)*. Raleigh, NC: North Carolina State University.